Solid-State Electronics 54 (2010) 235–242

Contents lists available at ScienceDirect

Solid-State Electronics

journal homepage: www.elsevier.com/locate/sse

Transmission line characterization on silicon considering arbitrary distribution of the series and shunt pad parasitics

Reydezel Torres-Torres [a,*], Rafael Venegas [b], Stefaan Decoutere [b]

[a] Instituto Nacional de Astrofísica, Óptica y Electrónica (INAOE), Department of Electronics, Tonantzintla, Puebla 72840, Mexico
[b] Interuniversity Micro-Electronics Center (IMEC), B-3001 Leuven, Belgium

ARTICLE INFO

Article history:
Received 12 March 2009
Received in revised form 27 August 2009
Accepted 8 September 2009

The review of this paper was arranged by Prof. S. Cristoloveanu

Keywords:
Interconnect
De-embedding
Transmission lines
Microwave measurements

ABSTRACT

This paper presents an analytical method to simultaneously determine the complex characteristic impedance and the pad parasitics of transmission lines fabricated on silicon. The method uses experimental two-port network parameters of two lines differing in length without the need of a reflect standard such as that required in TRL-like formulations. Furthermore, the losses associated with the silicon substrate are accurately considered using the experimentally determined complex propagation constant of the lines and three different configurations for the pad parasitics can be assumed. When using the extracted parameters in a model to represent transmission lines, excellent agreement between simulated and experimental data was achieved up to 50 GHz even for lines with lengths different to those used in the determination process.

1. Introduction

Characterizing and modeling on-chip transmission lines is of great importance when designing, implementing and measuring solid-state circuits and devices at high-frequencies. Perhaps the most common application of these lines is serving as interconnection channels in ICs. However, transmission lines also play an important role when performing microwave measurements [1,2], and when experimentally obtaining material and structure parameters [3,4]. For this reason, several methods to determine the fundamental parameters of transmission lines have been reported, which is due to the fact that the equivalent circuit model of a transmission line can be implemented once that the propagation constant (γ) and the characteristic impedance (Z_c) are known [5,6]. Whereas the accurate extraction of γ can be carried out in a simple way [7], the determination of Z_c represents a considerable challenge due to the difficulty to obtain the experimental reference impedance when using conventional thru-reflect-line (TRL) calibration algorithms. For this reason, the popular method proposed in [8] is commonly used to obtain Z_c of transmission lines fabricated in low-loss substrates. Unfortunately, this simple method is not applicable to lines fabricated over silicon due to the loss mechanisms associated with this type of substrate [9]. This has motivated the proposal of different methodologies to obtain Z_c: using a calibration comparison [10–12], simplifying the model for the pad parasitics [13–15], requiring structures with restricted dimensions [16,17], or using a fitting and optimization approach [18]. With the exception of the methods based on calibration comparisons, none of the reported approaches can be applied to accurately characterize transmission lines fabricated on lossy substrates and presenting arbitrary complex impedances as series and shunt pad parasitics, which is the typical case when implementing lines on RF CMOS. Unfortunately, when using a calibration comparison to obtain Z_c, on-wafer reflect standards are required in addition to the transmission lines to be characterized, which take precious space within a test chip and may not be always available.

In order to provide an alternative way to accurately characterize transmission lines fabricated on silicon substrates, in this paper we present an analytical and generalized method to obtain Z_c and the pad parasitics from measurements performed to two lines with different lengths. The method allows the simultaneous determination of these parameters while considering the substrate losses even when the pads-to-transmission line transition is not symmetrical. Thus, the obtained data can be used to implement models for transmission lines within an IC design or for measurement de-embedding purposes.

Before presenting the new method, a brief review of the most popular methods to characterize transmission lines without requiring the use of reflect dummy structures is presented.

* Corresponding author.
E-mail address: reydezel@inaoep.mx (R. Torres-Torres).

0038-1101/$ - see front matter © 2009 Elsevier Ltd. All rights reserved.
doi:10.1016/j.sse.2009.09.004

2. Simplified approaches

2.1. Assuming low dielectric losses

This approach relies on the fact that the distributed resistance (R), inductance (L), conductance (G), and capacitance (C) per unit length associated with the equivalent circuit model of a transmission line can be related to the product and quotient of γ and Z_c as [5]:

$$\gamma Z_c = R + j\omega L \tag{1}$$

$$\frac{\gamma}{Z_c} = G + j\omega C \tag{2}$$

where ω is the angular frequency and $j^2 = -1$. Thus, assuming that the lines are fabricated over a lossless substrate (i.e. $G = 0$), the complex Z_c can be obtained after solving (2); this is:

$$Z_c = \frac{\beta}{\omega C} - j\frac{\alpha}{\omega C} \tag{3}$$

In this equation, $\gamma = \alpha + j\beta$ can be accurately obtained from measurements performed to two lines of different lengths [7] and C can be estimated either from a curve fitting at low frequencies or from calculations [8]. In fact, this method is very accurate for low-loss substrates and was applied in [6] to characterize SiGe transmission lines fabricated in a fused silica substrate up to 110 GHz. However, due to the high losses associated with a silicon substrate, this method cannot be applied in this case since Z_c is expressed as:

$$Z_c = \frac{\beta}{\omega C} - \frac{G(\beta G - \omega\alpha C)}{\omega C(G^2 + \omega^2 C^2)} - j\left[\frac{\alpha}{\omega C} - \frac{G(\alpha G + \omega\beta C)}{\omega C(G^2 + \omega^2 C^2)}\right] \tag{4}$$

After comparing Eqs. (3) and (4), it is observed that determining Z_c using (3) yields severe deviations from the actual value of this parameter when G is not negligible. This is the case in silicon substrates.

2.2. Using single line measurements

Traditionally, when characterizing transmission lines, the associated experimental S-parameters are converted to the $ABCD$-parameters. In this case, the $ABCD$ matrix of a line with length l_n is expressed as [5]:

$$\mathbf{T}_n = \begin{bmatrix} A_n & B_n \\ C_n & D_n \end{bmatrix} = \begin{bmatrix} c_n & Z_c s_n \\ Z_c^{-1} s_n & c_n \end{bmatrix} \tag{5}$$

where $c_n = \cosh(\gamma l_n)$, $s_n = \sinh(\gamma l_n)$, and the subscript n is used to distinguish between lines of different lengths. Thus, Z_c can be obtained as:

$$Z_c = \sqrt{\frac{B_n}{C_n}} \tag{6}$$

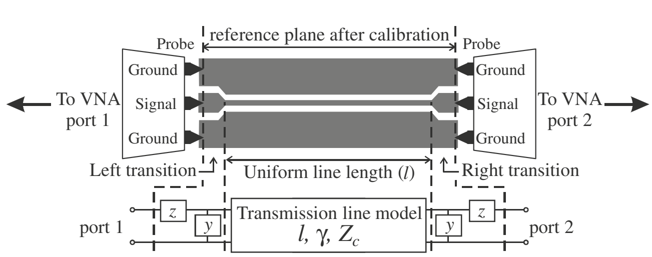

Fig. 1. Setup used to measure a CPW and the corresponding equivalent circuit model.

Even though this approach can be used when the substrate losses are not negligible, the pad parasitic effects associated with an actual measurement setup, as the one shown in Fig. 1, are still not considered. These parasitics are neglected in (5), which originates unexpected fluctuations on the real and imaginary parts of Z_c when plotting Eq. (6) versus frequency [18].

2.3. Using a simplified model for the pad parasitics

In order to consider the effect of the pad parasitics on the experimental $\mathbf{T}_n$, error matrices are used to represent the electrical transitions from the probes to the uniform transmission line (UTL) section. On silicon, these transitions are typically represented by means of a shunt admittance y shown in the model depicted in Fig. 1, whereas the series impedance z is considered to be negligible [10,13]. Thus, in order to correct the measurements from the error introduced by the shunt parasitics, the $ABCD$ matrices ($\mathbf{T}_1$ and $\mathbf{T}_2$) of two lines differing in length are multiplied in such a way that the matrix $\mathbf{M}$ is defined as:

$$\mathbf{M} = \mathbf{T}_1\mathbf{T}_2^{-1} \tag{7}$$

Afterwards, $\mathbf{M}$ is converted to the corresponding Y-parameter matrix $\mathbf{Y}$, which is given by:

$$\mathbf{Y} = \begin{bmatrix} Y_{11} & Y_{12} \\ Y_{21} & Y_{22} \end{bmatrix} = \mathbf{Y}_C + \begin{bmatrix} y & 0 \\ 0 & -y \end{bmatrix} \tag{8}$$

where $\mathbf{Y}_C$ is the Y-parameter matrix corrected from the effects of the shunt parasitics. Hence, the following matricial operation is applied to obtain $\mathbf{Y}_C$ [13]:

$$\mathbf{Y}_C = \frac{1}{2}\left\{\begin{bmatrix} Y_{11} & Y_{12} \\ Y_{21} & Y_{22} \end{bmatrix} + \begin{bmatrix} Y_{22} & Y_{21} \\ Y_{12} & Y_{11} \end{bmatrix}\right\}. \tag{9}$$

Once that $\mathbf{Y}_C$ is known, it can be converted to the corresponding $ABCD$-parameter matrix, which is assumed to be corrected from the pad parasitics, allowing to apply (6) to obtain Z_c.

As shown later in this paper, taking into account the shunt parasitics improves the extraction of Z_c in comparison with the approach that neglects the pad parasitics at all. However, the parasitic series impedance z can be considerable and introduce errors in the transmission line characterization process [11]. This is due to the fact that, in accordance with the model shown in Fig. 1, the experimental matrix $\mathbf{Y}$ after considering y and z is given by:

$$\mathbf{Y} = \left\{\left(\mathbf{Y}_C + \begin{bmatrix} y & 0 \\ 0 & -y \end{bmatrix}\right)^{-1} + \begin{bmatrix} z & 0 \\ 0 & -z \end{bmatrix}\right\}^{-1} \tag{10}$$

Notice that once z is included in the analysis, (9) lacks of validity and additional data processing is required. In addition, although the matricial operations applied in (10) are very simple, the determination of $\mathbf{Y}_C$ cannot be carried out in a direct way since the experimental data associated with the pad parasitics are not easily separable. This originates that, even though (10) is similar to those equations used in step-by-step de-embedding algorithms (e.g. those applied in test fixtures for probing relatively small devices) [2], these methods are not directly applicable for the case of transmission lines unless y and z are known *a priori*.

3. Formulation of the new method

The model shown in Fig. 1 corresponds to a UTL embedded between two identical coplanar waveguide (CPW) adapters as that shown in Fig. 2a. In contrast to previously reported approaches, this model considers the series and parallel pad parasitics as general impedance (z) and admittance (y) elements respectively. Whereas y represents the effective capacitive effects between the

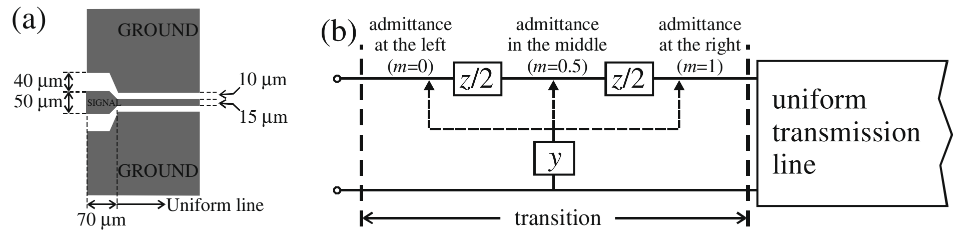

Fig. 2. (a) Transition used to feed the fabricated CPWs and (b) corresponding model for the three analyzed cases.

signal pad and the ground pads, z is associated with the inductance between the probe tips and the transmission line. As discussed in [11], there is an error on the extracted value for Z_c depending on how z is assumed to be distributed along the pad. Thus, although the common practice is considering that z is equally distributed at both sides of y in order to assume the symmetry condition required to apply the methods in [13–15,18], this is not always the best choice. For this reason, notice in Fig. 2b, that the proposed model for the transition can be used for several distributions of z along the pad depending on the value selected for m as explained later. Furthermore, in other approaches the use of an impedance transformer is required in the model of the test fixture since the UTL is simply represented by means of γ and l [10,11]. In our case, however, the transformer is not necessary since the effect of Z_c is considered in the model for the UTL, allowing to simplify the analysis as shown hereafter.

The method proposed here requires two lines differing only in length and embedded between transitions as shown in Fig. 1. Thus, the experimental *ABCD*-parameters of these lines can be expressed by the following equation:

$$\mathbf{T}_{Xn} = \mathbf{X}_L \mathbf{T}_n \mathbf{X}_R = \begin{bmatrix} A_{Xn} & B_{Xn} \\ C_{Xn} & D_{Xn} \end{bmatrix} \tag{11}$$

where the subscript n is used to distinguish between line 1 and line 2 parameters, the matrices $\mathbf{X}_L$ and $\mathbf{X}_R$ are associated with the left and right transitions respectively, and $\mathbf{T}_n$ is defined in (5).

In (5), c_n and s_n incorporate the propagation effects of the transmission line, including the losses and delay. Also notice that the line lengths are known and the complex value for γ can be obtained from S-parameter measurements performed to two lines with different lengths and embedded between identical pad structures [7]. This allows the simple calculation of c_n and s_n, and reduces the unknowns at the right hand side of (5) to Z_c.

In order to express $\mathbf{X}_L$ and $\mathbf{X}_R$ in terms of the pad parasitics, a variation of the *ABCD*-matrices used to represent series and shunt admittances and available in many textbooks can be used [19]. Thus, in accordance with the model shown in Fig. 2b, and assuming that the left and right transitions are identical but one rotated 180° with respect to the other, the associated matrices are:

$$\mathbf{X}_L = \begin{bmatrix} 1 + mzy & z + m(1-m)z^2 y \\ y & 1 + (1-m)zy \end{bmatrix} \tag{12}$$

$$\mathbf{X}_R = \begin{bmatrix} 1 + (1-m)zy & z + m(1-m)z^2 y \\ y & 1 + mzy \end{bmatrix} \tag{13}$$

where m can take values of 0, 0.5, and 1 depending on the desired distribution for the parasitics in the model for the pad (see Fig. 2b). These cases have been separately analyzed in the literature depending on the more suitable model for the transition used to probe the transmission line. The advantage of the characterization method proposed here is that one single algorithm can be used to obtain the unknown parameters and representing the complete structure in a consistent way.

When substituting (5), (12), and (13) into (11), an expression for A_{Xn} is found, this is:

$$A_{Xn} = a c_n + b s_n \tag{14}$$

where a is given by:

$$a = 2(m - m^2)(yz)^2 + 2yz + 1, \tag{15}$$

and b depends on m, y, z, and Z_c.

In order to determine a, the experimental data corresponding to the two lines is used to establish a linear equation system based on (14), this is:

$$A_{X1} = a c_1 + b s_1 \tag{16}$$
$$A_{X2} = a c_2 + b s_2 \tag{17}$$

which can be solved to determine a from:

$$a = \frac{A_{X1} s_2 - A_{X2} s_1}{\Delta} \tag{18}$$

where $\Delta = c_1 s_2 - c_2 s_1$.

Once a is known and a value for m has been selected, the product yz can be obtained by solving Eq. (15). Since y and z are mainly capacitive and inductive respectively, the correct root of (15) has a negative real part.

An equation similar to (14) can be written for C_{Xn}, this is:

$$C_{Xn} = d c_n + e s_n, \tag{19}$$

where d and e are respectively given by:

$$d = 2y(1 + (1-m)yz) \tag{20}$$

$$e = y^2 Z_c + \frac{1}{Z_c}(1 + (1-m)yz)^2 \tag{21}$$

Thus, d and e can be found by solving the equation system based on (19) and the data corresponding to the two lines, which yields:

$$d = \frac{C_{X1} s_2 - C_{X2} s_1}{\Delta} \tag{22}$$

$$e = \frac{C_{X2} c_1 - C_{X1} c_2}{\Delta} \tag{23}$$

After determining d and the product yz, the parallel pad parasitic element can be directly calculated by solving (20); this is:

$$y = \frac{d}{2(1 + (1-m)yz)} \tag{24}$$

which allows the determination of Z_c by solving a quadratic equation derived from (21). This is expressed as:

$$y^2 Z_c^2 - e Z_c + (1 + (1-m)yz)^2 = 0 \tag{25}$$

As can be observed, y and Z_c have been simultaneously obtained using the exact matricial equations associated with a UTL embedded between two transitions represented by means of the model of Fig. 2b. In this case, the sign ambiguity associated with (21) is re-solved considering that $\mathrm{Re}(Z_c)$ presents positive values continuous when plotted versus frequency, which are close to the designed impedance of the transmission line.

In order to obtain z, an expression for B_{Xn} is written as:

$$B_{Xn} = f\,c_n + g\,s_n \tag{26}$$

where:

$$f = 2z(1 + myz)(1 + m(1 - m)yz) \tag{27}$$

and g depends on m, y, z, and Z_c.

The coefficients f and g can also be determined from the solution of a linear equation system. Thus, associating the data of the two lines with (16) and solving to obtain f yields:

$$f = \frac{B_{X1}s_2 - B_{X2}s_1}{\Delta} \tag{28}$$

which allows the determination of z after solving (27), this is:

$$z = \frac{f}{2(1 + myz)(1 + m(1 - m)yz)} \tag{29}$$

4. Experimental verification

Several CPWs with different lengths and terminated at both sides with the transition shown in Fig. 2a were fabricated in a p-type silicon substrate with a resistivity of 20 Ω cm. The stripes were formed with aluminum having a sheet resistance of about 40 mΩ/square. The experimental *ABCD*-parameters of these lines were obtained from measured *S*-parameters using the corresponding two-port network parameter conversion. The measurements were performed using a previously calibrated vector network analyzer (VNA) and ground-signal-ground (GSG) coplanar probes with a pitch of 150 µm. The VNA calibration was performed to establish the measurement plane at the end of the probe tips and the *S*-parameter reference impedance at 50 Ω. In addition, the propagation constant of the lines was obtained as in [7] so that the new method can be applied.

The method was applied to the experimental *ABCD* matrices corresponding to two CPWs with lengths of 500 µm and 250 µm respectively. For the case of the proposed method, Z_c and the pad parasitics (i.e. y and z) were simultaneously determined assuming the different transition representations depicted in Fig. 2b. In Fig. 3 the real and imaginary parts of Z_c are plotted versus frequency for the three cases covered in this paper: assuming that the series impedance is located after the shunt admittance ($m = 0$), assuming that this impedance is evenly distributed at the right and left sides of the admittance ($m = 0.5$), and assuming that the impedance is located before the admittance ($m = 1$). Notice in these plots that, although the curves obtained in the three cases present almost the same values below 20 GHz, beyond this frequency a difference becomes apparent. This is due to the fact that as the frequency increases the second order terms in the Eqs. (12) and (13) also increase yielding variations in the extracted Z_c. Thus, Fig. 3 shows that assuming $m = 0$ results in smaller values for $\mathrm{Re}(Z_c)$ and bigger values for $\mathrm{Im}(Z_c)$ when compared with the other two cases, whereas the opposite occurs when assuming $m = 1$.

In order to determine m, a 2-port network model as the one shown in Fig. 1 was implemented in the Advanced Design System (ADS) circuit simulator of Agilent and compared with experimental data. In this model, the experimental data obtained for z, y, and Z_c for the three considered distributions of the pad parasitics ($m = 0$, 0.5, and 1) were used. With this model, the *S*-parameters of a line with length $l = 6400$ µm were obtained by performing the corresponding frequency domain simulations. The reason for using this relatively long line is to observe in an accentuated way the error introduced by the models. The results of the simulations are compared with experimental data in Fig. 4. As can be seen in this figure, although the insertion loss ($|S_{21}|$) is well represented considering the three cases, the return loss ($|S_{11}|$) is better reproduced when using $m = 1$ and this value is used in what follows.

An interesting point to be remarked here is the fact that the adequate value for m depends among other things on the structure of the transition and the probe position while performing the *S*-parameter measurements. For instance, placing the probes at different distances from the edge of the pads may yield substantial inductance variations [20], which consequently introduces differences in the position of the shunt capacitance within the model. Thus, consistent probe positioning is necessary for physically meaningful parameter extractions when using line-line algorithms. Additionally, the configuration and structure of the pads determines the most appropriate value for m. For example, when using microstrips a considerable series inductance is introduced by the ground pads [21], which is dependent on the number of vias used to interconnect these pads with the ground plane. In this case, m will also be dependent on the position of these vias and a straightforward way to determine the most appropriate value for this parameter is using a simulation-experiment correlation such as that shown in Fig. 4.

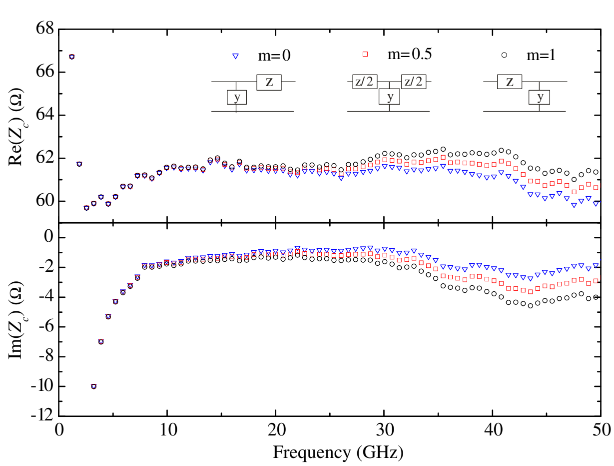

Fig. 3. Extracted characteristic impedance obtained for the three different distributions assumed for the transition elements. Notice the different scales.

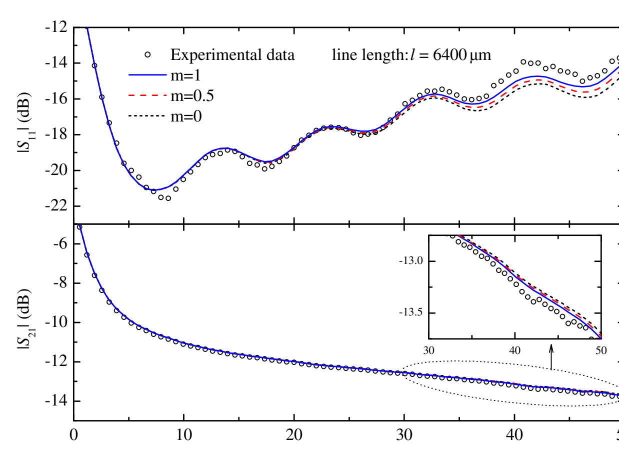

Fig. 4. Comparison between the experimental and simulated return and insertion losses using the data extracted considering different distributions of the pad parasitics.

Once that γ and Z_c are determined, (1) and (2) can be used to obtain the electrical parameters per unit length of the analyzed lines. The results are shown in Fig. 5. Notice the difference in L, C, R, and G depending on value of m used to extract Z_c. This difference is accentuated as frequency increases and an incorrect selection on m may introduce substantial differences in these electrical parameters and consequently in the corresponding transmission line model of a practical interconnect. In Fig. 5b, G and R are plotted up to 30 GHz since above this frequency the corresponding data become very noisy due to the difficulty to accurately determine the phase of Z_c at high frequencies (i.e. when $\mathrm{Re}(Z_c) \gg \mathrm{Im}(Z_c)$) [10].

In addition, a comparison with the methods discussed in Section 2 was carried out and presented in Fig. 6. As can be seen in this figure, the $\mathrm{Re}(Z_c)$ versus frequency curve presents an accentuated unphysical valley when the data is extracted assuming that the pad parasitics can be represented by means of a shunt admittance as in [13]. This valley becomes even more noticeable when using single line measurements and neglecting the pad parasitics. In contrast, in the curve associated with the data extracted with the new method using $m = 1$ the unphysical trend is almost removed. For a complete removal of this valley, more complicated models considering additional effects in the signal and ground pads have to be implemented [21].

Observe in Fig. 6 that neglecting the substrate losses as in [8] yields the $\mathrm{Re}(Z_c)$ versus frequency curve to deviate from the extractions performed with the other studied methods, which is due to the error introduced by neglecting G in (3). Furthermore, using this method results in a considerable underestimation of the $\mathrm{Im}(Z_c)$ data. For the case of the method in [13], the difference with the new method is noticeable in the extraction of $\mathrm{Im}(Z_c)$ up to about 15 GHz, whereas neglecting the pad parasitics yields even positive values for $\mathrm{Im}(Z_c)$, which is unexpected for lines fabricated on silicon substrates.

In order to verify the validity of the proposed methodology, simulations were performed using the extracted data assuming m=1 and the ADS circuit simulator. The results are shown in Fig. 7. Notice the excellent simulation-experiment correlation for a line with length l = 1450 μm. An important point to be remarked is the fact that even though this line was not used in the parameter extraction process, the simulations based on the new method reproduce the experimental data with accuracy. Conversely, when performing the simulations either using a single shunt admittance to represent the pad parasitics or neglecting these parasitics at all, there are significant deviations in the simulated insertion loss ($|S_{11}|$) and return loss ($|S_{21}|$) of the lines. This suggests that considering both the series and shunt parasitics is necessary to accurately

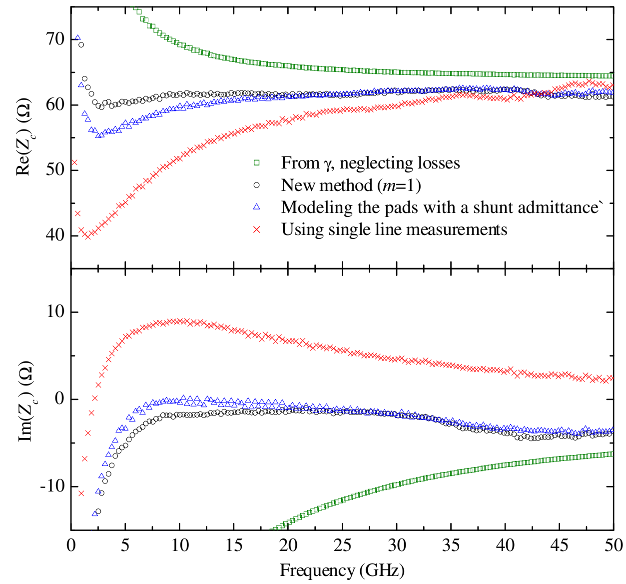

Fig. 6. Comparison between Z_c extracted using the new method and some popular extraction methods.

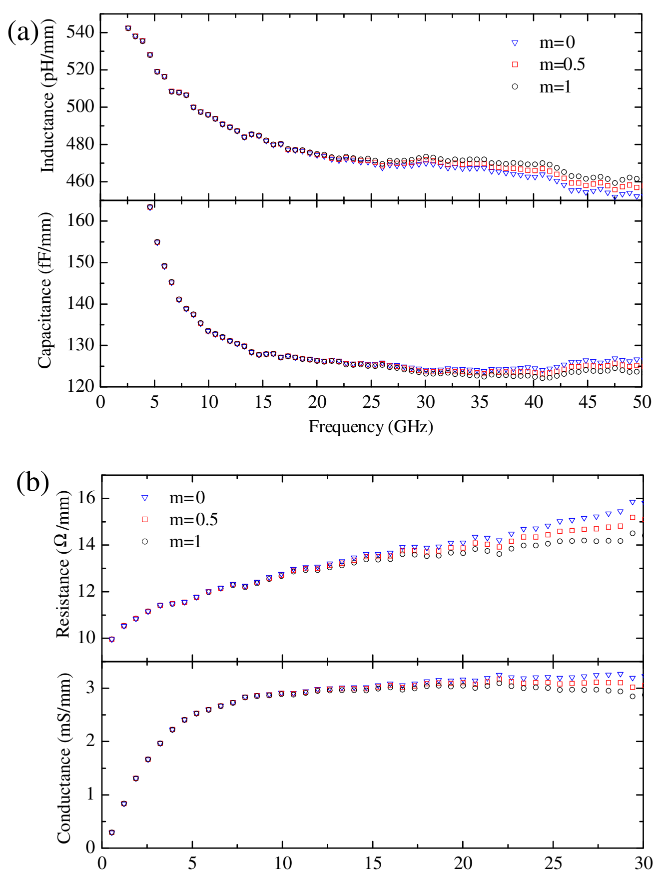

Fig. 5. Electrical parameters per unit length of the characterized transmission lines. The data was obtained from γ and the extracted Z_c using the new method considering different distributions of the pad parasitics: (a) inductance and capacitance and (b) resistance and conductance.

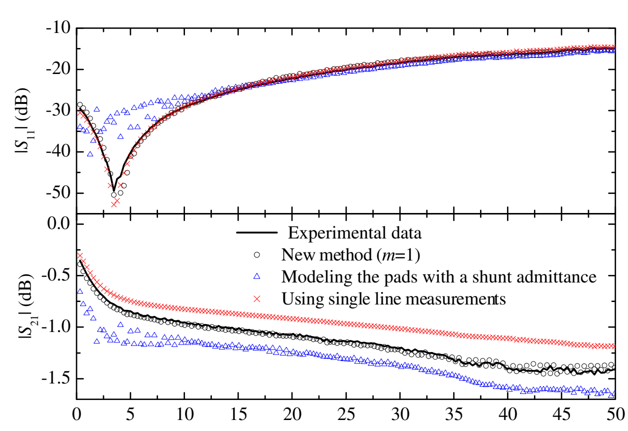

Fig. 7. Simulated and experimental return and insertion losses for a line with l = 1450 μm. The simulations were performed using the extracted parameters obtained using the new method, neglecting the series pad parasitics, and using single line measurements.

represent the effect of the pads when characterizing transmission line structures on silicon.

Since Z_c, y, and z determined with the new method allow the correct representation of the lines, these parameters can be used with de-embedding purposes in structures fed with CPWs. This is a common case when probing devices on-wafer. As a final remark on the length of the lines used throughout the characterization procedure, the difference in length between line 1 and line 2 has to be so different that allows the proper solution of the systems of linear equations associated with (14), (19), and (26). Otherwise, when $l_1 \approx l_2$ the equations in these systems become linearly dependent and no solution can be found. Fortunately, the same lines used for the experimental determination of γ as in [7,22] can be used in the proposed characterization method.

5. Modelling the pad parasitics

In accordance to previously developed models [11,18,19], the series and shunt pad parasitics present mainly inductive and capacitive effects respectively. However, in addition to these effects, the losses related to the inherent resistance of the substrate and metal used to form the lines influence the values of y and z. Taking this into consideration, an equivalent circuit can be used to represent y and z [2]. Thus, experimentally determining the equivalent circuit elements that represent y and z allows to demonstrate the feasibility of obtaining a physically meaningful model for the pad parasitics by using the proposed extraction method. This is shown hereafter.

Fig. 8 shows the equivalent circuit model of a GSG pad system including the finite resistance of the pads and the resistive coupling through the substrate. When analyzing this circuit as a two-port network, it can be demonstrated that the equivalent circuits associated with the shunt admittance and the series impedance of the pad system are those shown at the bottom of Fig. 8, where the effective values of the corresponding elements are approximately given by: $C_{y1} \approx 2C_{SG}$, $C_{y2} \approx 2C_G C_S/(2C_G + C_S)$, $R_y \approx R_{subs}/2$, $L_z \approx L_S + L_G/2$, and $R_z \approx R_S + R_G/2$. Notice that in this particular case, the shunt elements are assumed to be located at the end of the pads ($m = 1$), but the same result is obtained for the other cases studied in previous sections. In addition, it is important to mention that this model presents a limited frequency range of validity and higher order effects have to be considered for extending this range. However, good results were obtained up to 30 GHz for the analyzed structures as shown hereafter.

In accordance to the equivalent circuit for y, the following equation can be written:

$$y = \mathrm{Re}(y_2) + j[\omega C_{y1} + \mathrm{Im}(y_2)] \tag{30}$$

where y_2 is the admittance associated with the series connection of R_y and C_{y2}. Thus, the real part of y can be rearranged as:

$$\frac{\omega^2}{\mathrm{Re}(y)} = \frac{1}{C_{y2}^2 R_y} + R_y \omega^2 \tag{31}$$

Observe that (31) can be seen as the equation of a line. Thus, when plotting the experimental $\omega^2/\mathrm{Re}(y)$ versus ω^2 data, R_y can be obtained from the slope of the corresponding linear regression, and therefore C_{y2} can be obtained from the intercept with the abscises. Since at relatively high frequencies $\mathrm{Re}(y) \ll \mathrm{Im}(y)$, this plot becomes noisy beyond a given frequency dependent on the substrate resistivity and the pad capacitances. For this reason, in Fig. 9a the linear regression is performed up to 5 GHz, allowing a proper extraction of R_y and C_{y2}.

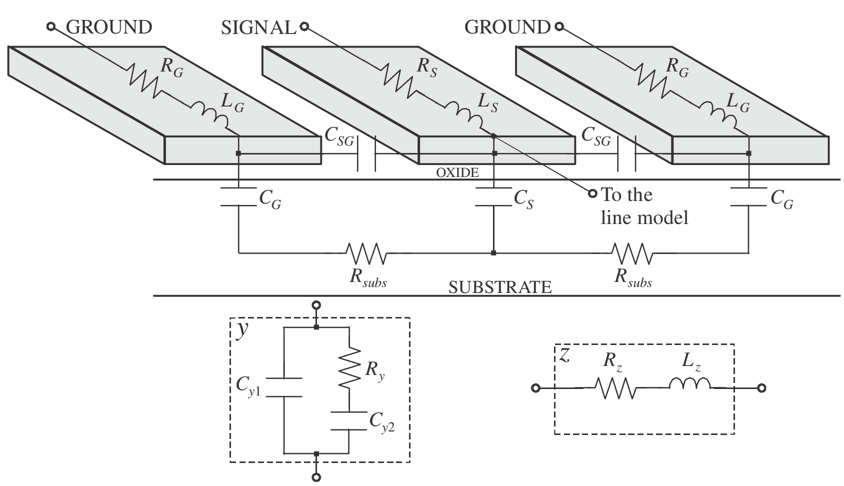

Fig. 8. Simplified model for a GSG pad system and the corresponding equivalent circuits for y and z.

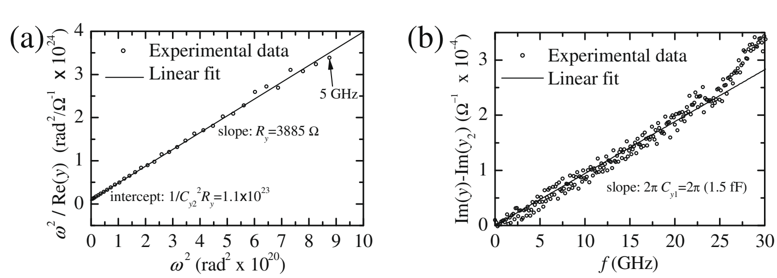

Fig. 9. Plots illustrating the extraction of: (a) R_y and C_{y2}, and (b) C_{y1}.

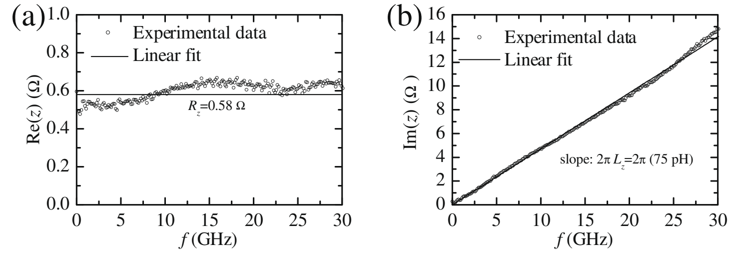

Fig. 10. Plots illustrating the extraction of: (a) R_z and (b) L_z.

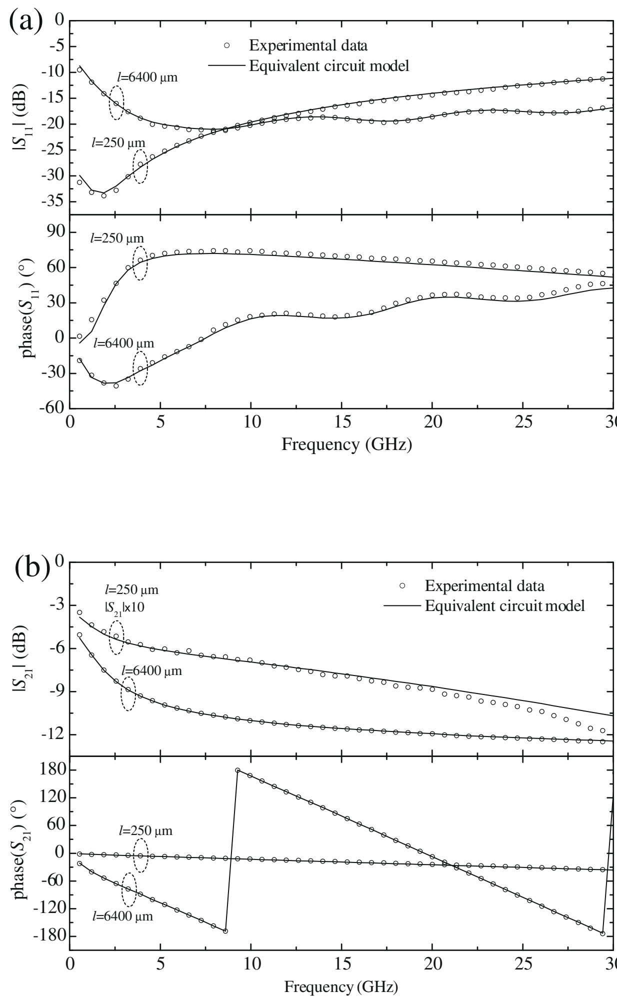

Fig. 11. Experimental *S*-parameters for two lines compared with the model using the extracted Z_c and the equivalent circuits for *y* and *z* assuming *m* = 1: (a) S_{11} and (b) S_{21}.

Once that R_y and C_{y2} are obtained, the imaginary part of y_2 can be computed from:

$$\mathrm{Im}(y_2) = \frac{\omega C_{y2}}{1 + (\omega C_{y2} R_y)^2} \quad (32)$$

Therefore, when solving (30) for $\mathrm{Im}(y) - \mathrm{Im}(y_2)$ yields:

$$\mathrm{Im}(y) - \mathrm{Im}(y_2) = \omega C_{y1} \quad (33)$$

In this equation, $\mathrm{Im}(y_2)$ is computed using (32), which allows to determine C_{y1} as illustrated in Fig. 9b.

For the case of *z*, the equation associated with the corresponding equivalent circuit is:

$$z = R_z + j\omega L_z \quad (34)$$

Thus, a straightforward determination of R_z and L_z can be carried out when plotting the experimental $\mathrm{Re}(z)$ and $\mathrm{Im}(z)$ versus frequency as illustrated in Fig. 10.

After determining all the equivalent circuit parameters for *y* and *z*, the 2-port network model shown in Fig. 1 was implemented again in ADS, but now substituting the blocks that represent *y* and *z* for the corresponding equivalent circuits. The simulated *S*-parameters for two lines with very different lengths are compared with experimental data in Fig. 11 showing an excellent agreement in magnitude as well as in phase up to 30 GHz. This demonstrates that the pad parasitics obtained using the proposed method allow the determination of physically meaningful parameters associated with the corresponding electrical behaviour.

6. Conclusions

An analytical methodology for characterizing transmission lines fabricated on silicon substrates has been proposed and verified. In addition, a comparison with other methodologies that use two lines to obtain the parameters associated with a transmission line was carried out. The proposed methodology allows the simultaneous determination of arbitrarily distributed pad parasitics and the characteristic impedance whereas considering the losses associated with a silicon substrate. These parameters can either be used with de-embedding or characterization purposes, which represents a valuable tool when measuring and characterizing devices and interconnects on-wafer.

Acknowledgements

The authors thank Svetlana Sejas and Víctor Vega for performing the measurements and Dr. Gerardo Romo for the useful discussions. This work was supported in part by CONACyT-Mexico.

References

[1] Tiemeijer LF, Havens RJ. A calibrated lumped-element de-embedding technique for on-wafer RF characterization of high-quality inductors and high-speed transistors. IEEE Trans Electron Dev 2003;50(March):822–9.
[2] Torres-Torres R, Murphy-Arteaga R, Reynoso-Hernandez JA. Analytical model and parameter extraction to account for the pad parasitics in RF-CMOS. IEEE Trans Electron Dev 2005;52(July):1335–42.
[3] Hinojosa J. *S*-parameter broadband measurements on-coplanar and fast extraction of the substrate intrinsic properties. IEEE Microw Wireless Comp Lett 2001;11(February):80–2.
[4] Leal-Romero R, Zuniga-Juarez JE, Zaldivar-Huerta IE, Maya-Sanchez MC, Aceves-Mijares M, Reynoso-Hernandez JA. Fabrication and characterization of coplanar waveguides on silicon using a combination of SiO_2 and SRO_{20}. IEEE Trans Compon Packag Technol 2008;31(September):678–82.
[5] Eisenstadt WR, Eo Y. *S*-parameter-based IC interconnection transmission line characterization. IEEE Trans Compon Packag Technol 1992;15(August):483–90.
[6] Zwick T, Tretiakov Y, Goren D. On-chip SiGe transmission line measurements and model verification up to 110 GHz. IEEE Trans Adv Packag 2000;23(August):470–9.

[7] Reynoso-Hernández JA. Unified method for determining the complex propagation constant of reflecting and nonreflecting transmission lines. IEEE Microw Wireless Comp Lett 2003;13(August):351–3.
[8] Marks RB, Williams DF. Characteristic impedance determination using propagation constant measurement. IEEE Microw Guided Wave Lett 1991;1(June):141–3.
[9] Lederer D, Raskin JP. Substrate loss mechanisms for microstrip and CPW transmission lines on lossy silicon wafers. Solid-State Electron 2003;47(November):1927–36.
[10] Williams DF, Arz U, Grabinski H. Accurate characteristic impedance measurement on silicon. MTT-S IMS Dig 1998:1917–20.
[11] Williams DF, Arz U, Grabinski H. Characteristic-impedance measurement error on lossy substrates. IEEE Microw Wireless Comp Lett 2001;11(July):299–301.
[12] Vandenberghe S, Schreurs DM, Carchon G, Nauwelaers BK, Raedt WD. Characteristic impedance extraction using calibration comparison. IEEE Trans Microw Theory Tech 2001;49(December):2573–9.
[13] Mangan AM, Voinigescu SP, Yang MT, Tazlauanu M. De-embedding transmission line measurements for accurate modeling of IC designs. IEEE Trans Electron Dev 2006;53(February):235–41.
[14] Zuniga-Juarez JE, Reynoso-Hernandez JA, Zarate-de-Landa A. A new method for determining the characteristic impedance Z_c of transmission lines embedded in symmetrical transitions. MTT-S IMS Dig 2008:52–5.
[15] Narita K, Kashta T. An accurate experimental method for characterizing transmission lines embedded in multilayer printed circuit boards. IEEE Trans Adv Packag 2006;29(February):114–21.
[16] Ng AC, Chua LH, Ng GI, Wang H, Zhou J, Nakamura H. Broadband characterisation of CPW transition and transmission line parameters for small reflection up to 94 GHz. Asia–Pacific Microw Conf Proc 2000: 311–5.
[17] Tretiakov Y, Rascoe J, Vaed K, Woods W, Venkatadri S, Zwick T. A new on-wafer de-embedding technique for on-chip RF transmission line interconnect characterization. ARFTG Conf Dig 2004:69–72.
[18] Post JE. On determining the characteristic impedance of low-loss transmission lines. Microw Opt Tech Lett 2005;47(October):176–80.
[19] Pozar DM. Microwave engineering. 3rd ed. New York: Wiley; 2005.
[20] Williams DF, Miers TH. De-embedding coplanar probes with planar distributed standards. IEEE Trans Microw Theory Tech 1988;36(December): 1876–80.
[21] Wiatr W, Walker DK, Williams DF. Coplanar-waveguide-to-microstrip transition model. MTT-S IMS Dig 2000:1797–800.
[22] Moukanda M, Ndagijimana F, Chilo J, Saguet P. Complex permittivity extraction using two transmission line *S*-parameter measurements. African Phys Rev 2008;2:62–4.